





Magnetic-electric dipole circularly polarized antenna with unidirectional radiation pattern with improved characteristics

Seied Ali Banihashem¹, Pejman Mohammadi²  and Yashar Zehforoosh² 

¹Department of Electrical Engineering, Urmia Branch, Islamic Azad University, Urmia, Iran and ²Microwave and Antenna Research Center, Urmia Branch, Islamic Azad University, Urmia, Iran

Research Paper

Cite this article: Banihashem SA, Mohammadi P, Zehforoosh Y (2023). Magnetic-electric dipole circularly polarized antenna with unidirectional radiation pattern with improved characteristics. *International Journal of Microwave and Wireless Technologies* 1–8. <https://doi.org/10.1017/S1759078723001393>

Received: 15 January 2023
Revised: 11 November 2023
Accepted: 15 November 2023

Keywords:

circular polarization; dipole; Magnetic-electric; wide impedance bandwidth

Corresponding author: Pejman Mohammadi;
Email: p.mohammadi@iaurmia.ac.ir

Abstract

In this paper, a compact unidirectional antenna consisting of a planar electric dipole and a shortened connecting element is introduced. This antenna is excited by a Γ -shaped feeding line. A wide impedance bandwidth in the frequency range of 1.3–3.3 GHz is observed in the output performance. Sufficient main lobe and low level back lobe have been introduced as other characteristics of the structure, based on radiation patterns. The antenna design process is evaluated step-by-step and using parametric study based on the antenna geometry. One of the main features of the desired antenna is the realization of circular polarization in a high percentage of the operational bandwidth 1.5–3.3 GHz. The radiation patterns of the orthogonal planes E-field and H-field along with the left-handed and right-handed circular polarization patterns for the desired antenna have been extracted and analyzed. A three-dimensional structure in the form of stacked stepped disks (SSD) is introduced to increase overall performance of antenna. There is an acceptable similarity between the E-field and H-field radiation patterns, which shows the accuracy of the design process. On the other hand, for studying the circular polarization, left-handed and right-handed patterns based on the main beam direction and orthogonal polarization level have acceptable performance. The maximum overall gain of the antenna in the designed frequency band is near to 13 dB.

Introduction

Due to the progress in new generations of telecommunications, such as 4.5G networks, broadband systems, and IEEE standards for local wireless networks and Internet of Things devices, demand for broadband antennas with gain improvement and unidirectional patterns are essential [1–5]. This type of antenna can be a suitable choice for wireless telecommunication, which electrically have unique behaviors that can be attributed to wide impedance bandwidth, low level of cross-polarization, good front to back ratio, relatively symmetrical radiation pattern, and stable gain in the desired frequency band [2]. Recently, many researches have been done on the introduction of unidirectional broadband systems and radiation elements related to it. A unidirectional antenna can be realized by placing a quarter-wavelength dipole surrounded by a defected ground surface [3]. Because the dimension of this type of antenna is measured in terms of wavelength and it depends on frequency, it has the disadvantage of large changes in gain and beam width at the operational bandwidth. One of the famous structures is using of microstrip antennas [4–6]. Many researches have been introduced for the design of broadband microstrip antennas, which include L-shaped probe feeding, aperture coupling, use of U-shaped slits, and parasitic appendages [4–8]. Many of these structures have a suitable impedance bandwidth for telecommunication applications for different types of IEEE standards. However, the weak points of these structures are low gain and the high cross polarization level at impedance bandwidth [9–11]. Although methods, such as eliminating the opposite phase, L-shaped couplings and feeding M-shaped couplings have been introduced to solve these defects, the main goal is to reduce the level of cross polarization and gain stabilization [8, 11, 12]. It can be concluded that the main challenge, is the changes of beam width with frequency in E and H planes. To achieve a relatively uniform radiation pattern in E and H planes and to have stable performance in the impedance bandwidth, the main idea is to use a self-complete antenna that has an electric dipole and a magnetic dipole [11]. The electric dipole has butterfly radiation pattern on the E plane, omnidirectional radiation pattern on the H plane [12], this theorem is true in the opposite case for a magnetic dipole. If both of these electric and magnetic dipoles are stimulated simultaneously by an appropriate amplitude and phase, a unidirectional radiation pattern similar to that in E and H planes can be obtained. Most of the structures introduced in this field are based on a combination of grooved and dielectric plates [8, 10–12], but the main

problem is the low impedance bandwidth. On the other hand, polarization is another important factor in determining the performance of telecommunication systems. In such a way that mismatching polarization will lead to multi-path fading and destructive effects of interference. The effect of multi-path reflections will lead to the change of polarization from left-handed to right-handed and vice versa. If both antennas on the transmitter and receiver have circular polarization characteristics, the aforementioned defects will not be considered as a design process [8, 13–19]. Planer and 3D microstrip antennas with circular polarization with relatively small dimensions are suitable and significant for wireless telecommunication systems. In these systems, these characteristics are obtained by different methods, most of which can be achieved by stimulating two orthogonal modes in the following methods [20–23]:

1. Application of T-shaped appendage perpendicular to the coplanar feeding line.
2. -Using L-shaped appendages in the ground corner of the slotted antenna.
3. -Applying gaps in the ground plane and using the parasitic element.

In this research, a new self-complementary electro-magnetic bipolar structure with relatively suitable gain and symmetrical radiation patterns in E and H planes has been introduced. The proposed structure consists of a quadratic wavelength cut-off plate and a plate dipole, which is equivalent to a combination of electric and magnetic structures. A three-dimensional structure in the form of stacked stepped disks (SSD) is introduced to increase overall performance of antenna. The proposed antenna structure is a suitable choice for wireless communication due to its good electrical performance. At the frequency bandwidth of the proposed antenna, several operational bands are covered based on the criteria of the Federal Communications Commission as follows: The frequency band (2.110–2.155 GHz) for fixed and mobile telecommunications, which is the downlink band, it should be noted that the 1.710–755 GHz band is also used for the uplink according to this standard, takes frequency band (2.2–2.290 GHz). This band is used for direct line of sight mobile telecommunications. Frequency band (2.320–2.345 GHz) for radio channels, applied frequency band for scientific and medical industries, in telecommunication industry for wireless networks under IEEE802.11, IEEE802.15.4 standard, and frequency band 2.655–2.690 GHz is used in the astronomical radio industry.

Antenna design

The proposed structure is based on the combination of electric and magnetic dipoles. Among the many structures for electric dipoles, a wide-band planar dipole with a short circuit resonator, which we consider as a magnetic dipole, is used in [22, 23] to combine these two antennas. The shortened connection is placed vertically and is connected to the plane dipole. Based on this topology, a new broadband antenna with a novel structure is obtained, which operates at an intermediate frequency of 2.5 GHz. Each part of an electric dipole has a width of half wavelength in free space and its length is a quarter of wavelength. The shortened resonator has a height of 30 mm, which is exactly equivalent to the length of the resonator. A method of using parasitic L-wires to form an electric dipole radiation is introduced to solve this unstable gain problem. It is well

known that the radiation pattern of a magnetic dipole is like an alphanumeric character “o” in the E-plane and “8” in the H-plane. In contrast, the radiation pattern of an electric dipole is figure “8” in the E-plane and a figure “o” in the H-plane. Once the planner modified patch (a source of electric dipole) and vertical quadrature wavelength shorted patch antenna (a source of magnetic dipole) are excited simultaneously with proper amplitudes and phases in between these two sources, the radiating power can be reinforced in the broadside direction but suppressed in the back side. In our case, since the electric- (j) and magnetic- (m) dipoles are excited from the shorted Γ -shaped feeding line, and the differences of amplitude and phase between the two sources are controlled by the values of L_6 and L_8 ; such that, it is expected that a unidirectional pattern with low back radiation can be achieved. As a result, the antenna in this proposed form finds an obvious advantage for stable gain over the frequency band due to the stable low back radiation across the operating bandwidth. At other hand, if the phase difference between the radiant elements is 90° or a multiple of 90° , a circular polarization is expected. On the other hand, if phase difference for a pair of radiant elements is excited in above method, circular polarization will be achieved. In order to provide two orthogonal modes of equal amplitude and 90° phase difference, the differential phase difference in length between two branches must be to provide 90° phase difference for the CP antenna. The phase difference of 90° between adjacent patches should be produced by adjusting the length of Γ -shaped feeding line, which means that the expected value in length between two branches must be to provide 90° phase difference. Finally, two orthogonal TE₀₁ and TM₁₁ modes are stimulated and the CP is realized. In order to access the broadband feature, the distance between two vertical planes is very important and is optimized by parametric analysis. The initial criterion for this value is something around 0.15 of wavelength, adapted from reference [22]. The key point of this design is choosing the size of the ground plane, which will strongly affect the radiation pattern. By carefully choosing this parameter, the radiation will be reduced to the minimum desired value. In order to feed the antenna, a Γ -shaped probe has been used, which consists of three interconnected metallized parts. The first vertical part is connected from the end to the coaxial cable and the ground plane. This section must have a characteristic impedance of 50 ohms in order to better impedance matching. The second part is placed horizontally parallel to the ground plane and connected to the previous part and is responsible for coupling electrical energy to the bipolar plate and the short circuit resonator. The circuit characteristics of this part can be realized by controlling the physical length. The important point is that this part strongly exhibits inductance properties and can affect the overall adaptation of the antenna. The third part, which is a vertical plane, is the same as the previous part. It is like an open circuit transmission line. A three-dimensional structure in the form of SSD is introduced to increase overall performance of antenna. Gain improvement over the operational bandwidth is achieved by using a SSD (high-permittivity dielectric). SSD is flat at the bottom and has a step-base profile on the top. Figure 1 shows general view of the proposed antenna in different dimensions with equipped with SSD structure. SSD is made of Rogers C10 dielectric material with permittivity of 10.2 with tolerance of 0.4 and loss tangent of 0.0023. Optimal final dimensions of the antenna are as follows (lengths are in mm): $L_1 = 150, L_2 = 150, L_3 = 30, L_4 = 44.5, L_5 = 30, L_6 = 40, L_7 = 58, L_8 = 16, L_9 = 32, L_{10} = 12, L_{11} = 25, R_1 = 20, R_2 = 40, R_3 = 60, R_4 = 80, H_1 = 10, H_2 = 10, H_3 = 10, \text{ and } H_4 = 10$.

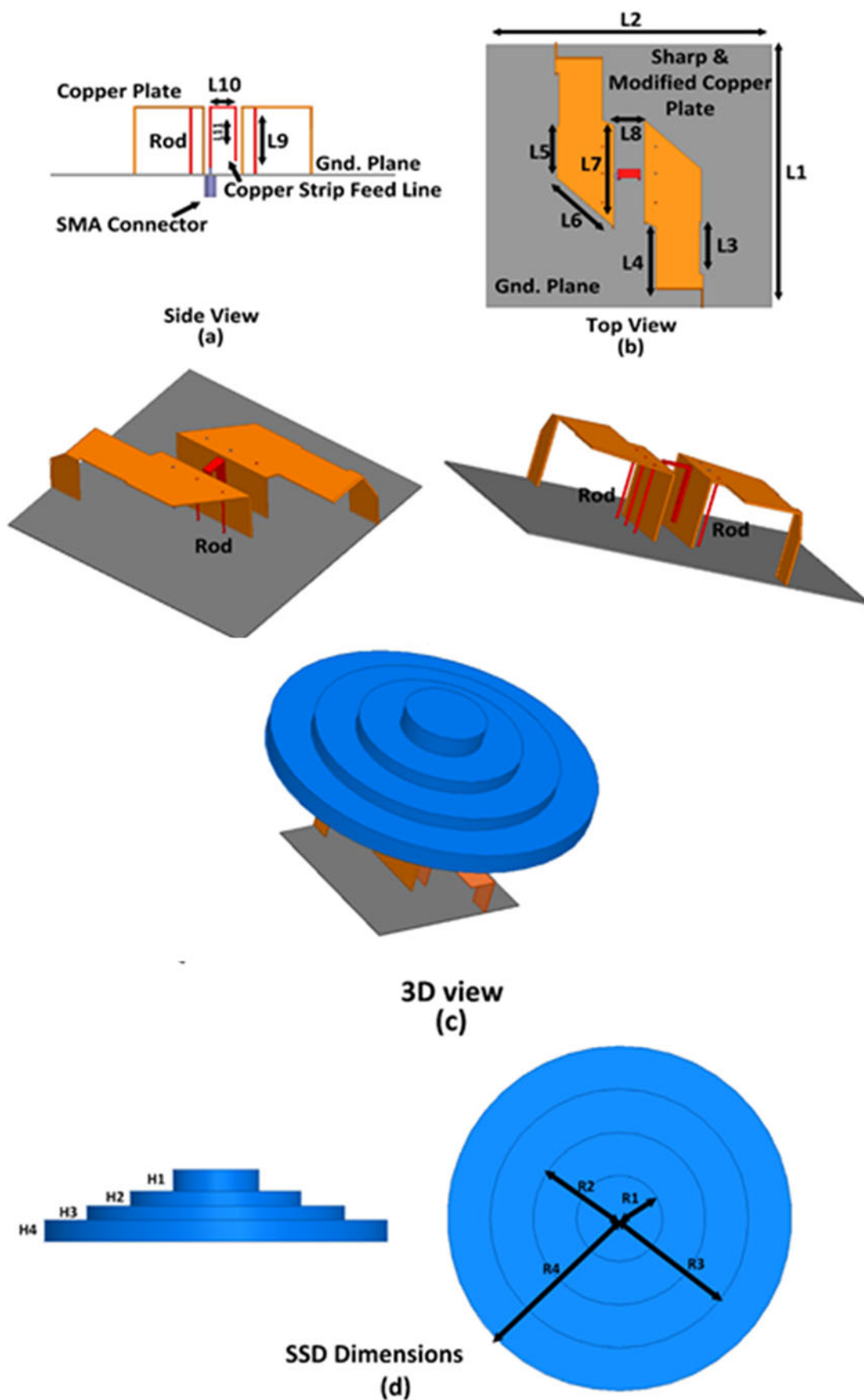


Figure 1. General view of the proposed antenna: (a) side view, (b) top view, (c) 3D view, and (d) SSD dimensions.

Results and discussion

The goal of this section, is investigating the main parameters effect on the performance of the antenna, which was done by HFSS simulator software. Figure 2 shows the return loss curve of the antenna based on the L_6 length variation. The length of the diagonal opening of the upper plate have the ability to control the resonance frequency is shown. It should be mentioned that to reach optimal operation, the trial and error process in designing should be done. Another parameter that has a great impact on setting the resonance frequency and overall bandwidth of the antenna is the horizontal distance between the two upper plates, which plays the role of the equivalent capacitor in the final resonant circuit due to the pairing of the two plates. In this design, the defected walls of the metallic reflector on parch as radiator have significant effects on the gain, AR, and impedance matching. Additionally, the defected walls not only enhance the gain, but it significantly improves the gain value. In order to achieve circular polarization performance, horizontal plates are chosen as electric dipole. Moreover, the effects of these plates are also evaluated for gain result. The value of gain with plates is more stable. A U-shaped feed structure is adopted between the radiation elements. This U-shaped feed can well excite the radiation elements by chosen a suitable width. Figure 3 reports the impedance bandwidth curve of the proposed antenna based on length of L_8 , as it is known that the length of the vertical stepped part of the screen has a great effect on the impedance bandwidth

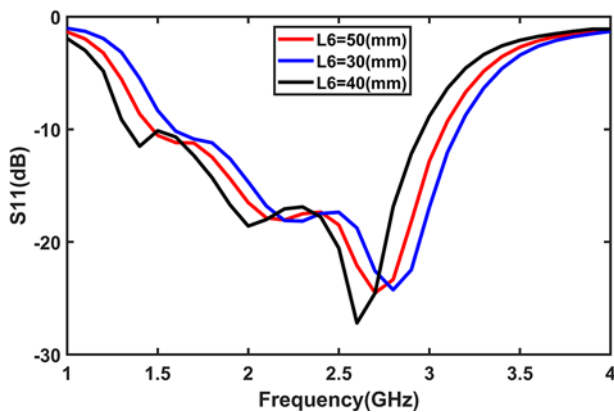


Figure 2. Return loss curve for L_6 length changes.

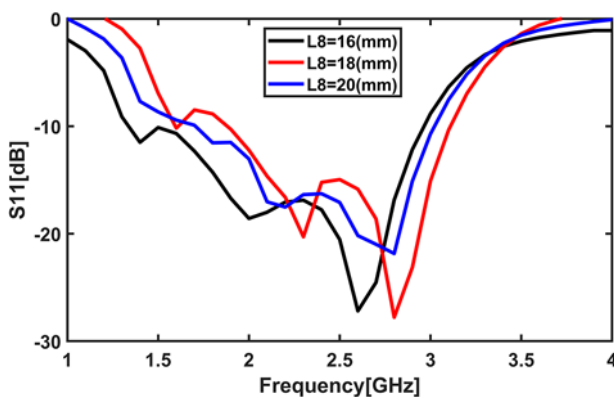


Figure 3. Return loss curve for L_8 length changes.

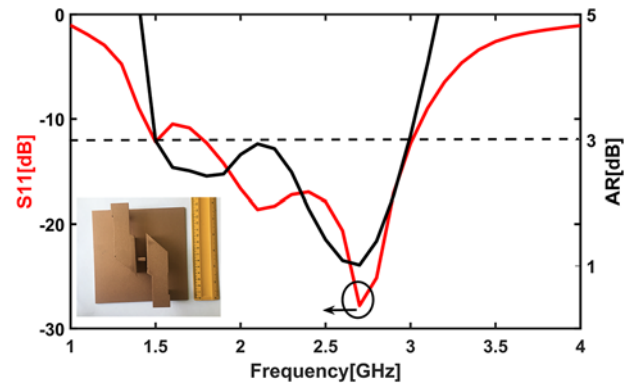


Figure 4. Return loss and AR with frequency variation with fabricated structure.

of the desired antenna, from this figure it is determined that the bandwidth It has expanded from 1.3 to 2.9 GHz and has a ratio of (80%). It should be noted that in all the previous diagrams obtained based on parametric studies, the optimal solutions are black curves. Figure 4 shows the curves of the return loss and axial ratio of the final antenna, as it is obvious that the antenna design process has an acceptable accuracy in terms of performance. This figure shows the axial ratio curve of the antenna, the proposed antenna in the frequency range of 1.5–2.9 GHz has the feature of circular polarization, which is considered the one of important feature of this antenna. In 95% ratio of the operational band, the circular polarization is realized. It should be noted that the presented antenna has relatively stable gain and radiation in the desired frequency range. Figure 5 shows radiation pattern of the circular polarization gain of the proposed antenna in left-handed and right-handed and E-field plane and H-field plane. This figure shows the radiation pattern of the antenna at 2.6 GHz frequency and E and H planes. As it is known, the width of the main beam in both mentioned fields are almost similar, which indicates the good performance of the antenna. It is also clear that the push of the curves on E and H pages are in the broadside mode and are very close to each other and are completely tangent to each other. It should be noted that the level of the back lobe is very small in both cases and the antenna radiation pattern measurement parameter is in good condition, which is less than 10 dB. Back lobe and SLL are acceptable. This figure shows the curve of left-handed and right-handed circular polarization radiation patterns at 2.6 frequency. In terms of beam angle and cross polarization level, the antenna has a relatively good condition. On the other hand, broadside radiation patterns are based and symmetrical in the frequency band. In order to improve the overall performance of the antenna, a structure with high permeability coefficients is placed at a distance of half a wavelength from the antenna radiation surface. The effect of assembling of stacked step based (SSD) layer as superstrate on the final antenna performance and evaluating the improvement are studied at next plots. For this purpose, the performance is studied in two cases without superstrate layer and with superstrate layer.

Figure 6 illustrates return loss curve of ultimate antenna without SSD and with SSD structures assembling. It is clear that the bandwidth in the state without SSD expands from 1.3 to 2.9 (76%), so that with the aforementioned superstrate layer, the bandwidth will be from 1.3 to 3.3 GHz (87%). So, an improvement of nearly 400 MHz or 11% of fractional impedance bandwidth is obtained. Figure 7(a) and (b) shows the simulated and measured axial ratio

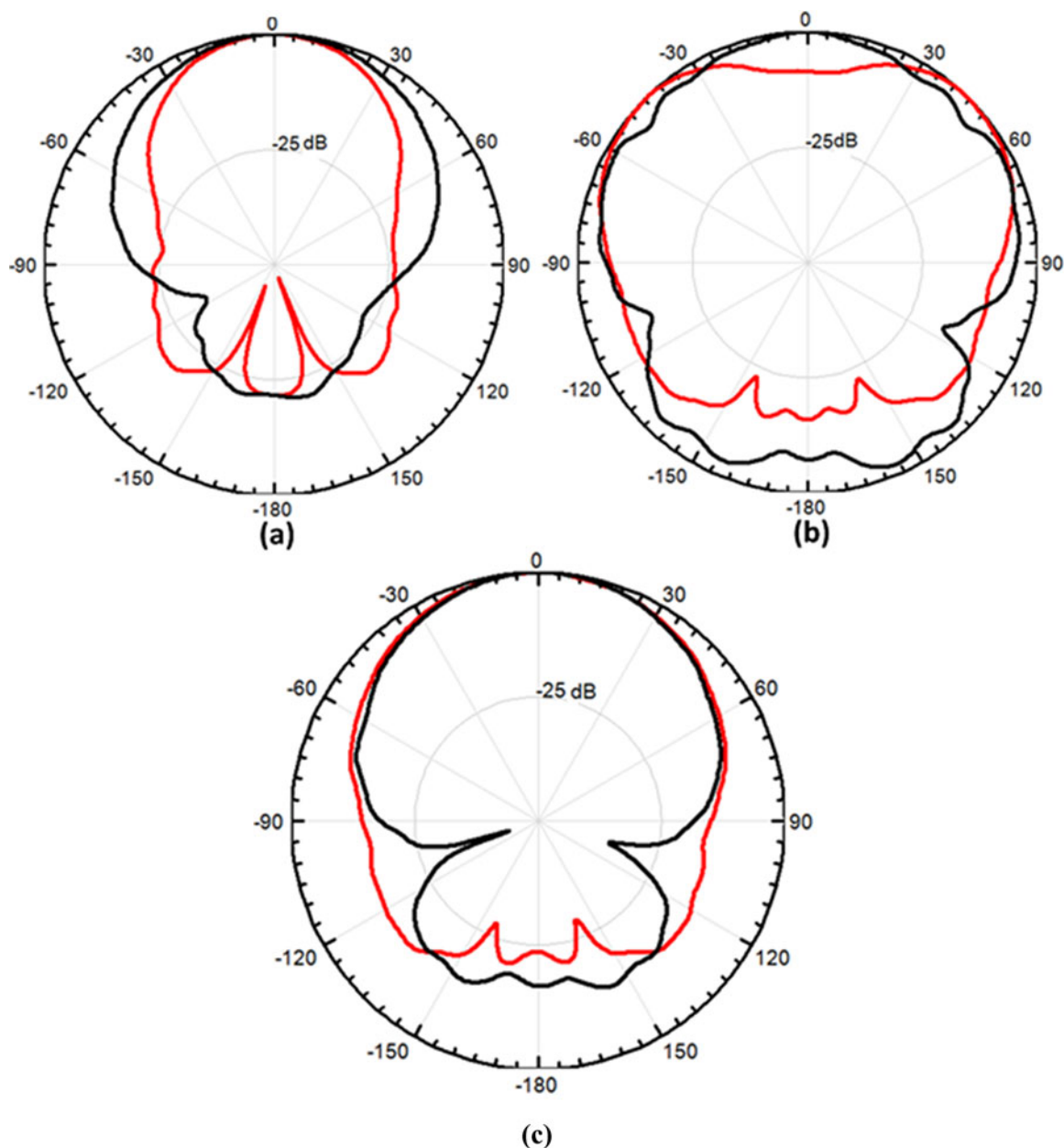


Figure 5. The measured radiation pattern of the circular polarization gain of the proposed antenna @ 2.6 GHz: (a) left-handed and (b) right-handed. (c) The measured radiation pattern of the proposed antenna in electric and magnetic field planes (black: E-field plane and red: H-field plane).

curves of ultimate antenna without SSD and with SSD structures assembling, respectively. There is good correlation among the results and little deviation leads from fabrication tolerance and non-ideal SMA. It shows the change curve of the axial ratio of the antenna with the frequency for the two mentioned states. ARBW is extended between 1.5 and 2.9 GHz for the state of without SSD and 1.5 and 3.3 GHz for state of with SSD. From this figure, it is clear that the circular polarization bandwidth is improved by nearly 12%, and as a result, it can be understood that CP is achieved in almost all the applied bands, and this means is that the CP purity has increased to a large extent, which is one of the main advantages of the proposed antenna. Figure 8 shows extracted return loss of ultimate antenna, there is good correlation between simulated and measured parameter. It is clear that impedance bandwidth is

between 1.3 and 3.3 GHz (87%). Figure 9(a) and (b) shows the simulated and measured curves of gain variation with frequency for two cases (with SSD and without SSD). It is quite obvious that the use of the SSD layer leads to the stabilization of the antenna gain linearly in the working bandwidth of the antenna. It should be noted that the maximum gain of 13 dB was measured, which is comparable. In case of no layer, we have about 3 dB increase in gain. It should be mentioned again that the main effect of this layer is to stabilize the gain in operational bandwidth. Figure 10 shows left-handed and right-handed curves at 2.8 GHz frequency. A good coronation is observed in output results, sufficient SLL and isolation of left-handed and right-handed patterns. The maximum value of right-handed pattern in $\theta = 0^\circ$ and for left-handed $\theta = -180^\circ$ (see Figure 11). Table 1 shows the comparison of the proposed

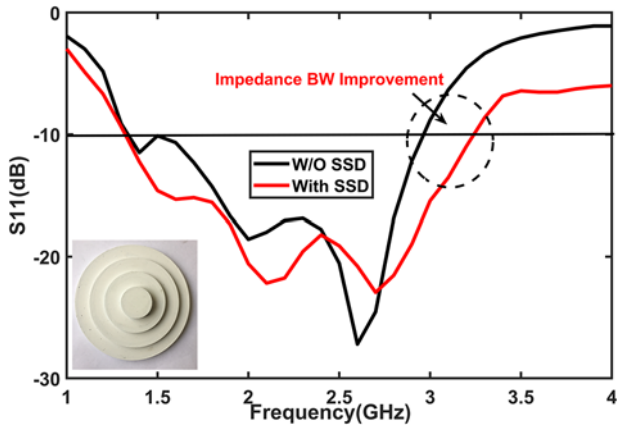


Figure 6. Return loss curve of ultimate antenna without SSD and with realized SSD structures assembling.

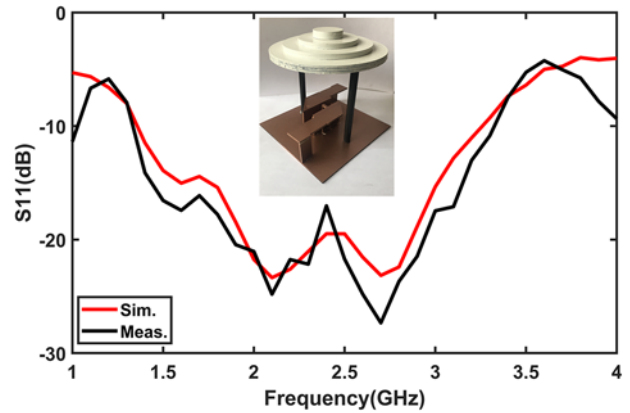


Figure 8. Extracted return loss of ultimate fabricated antenna.

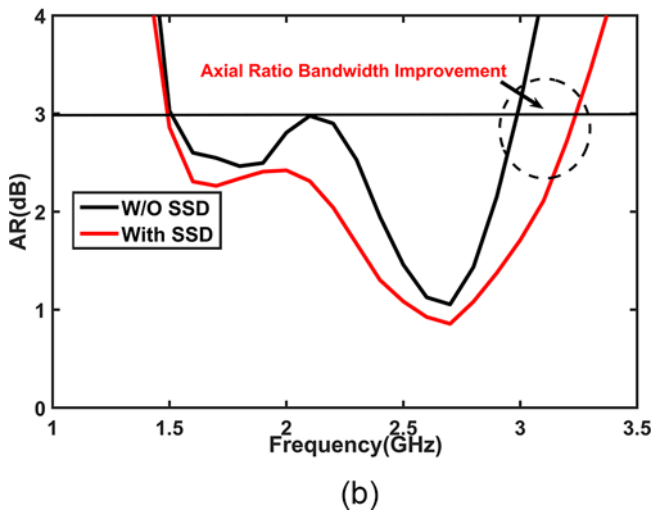
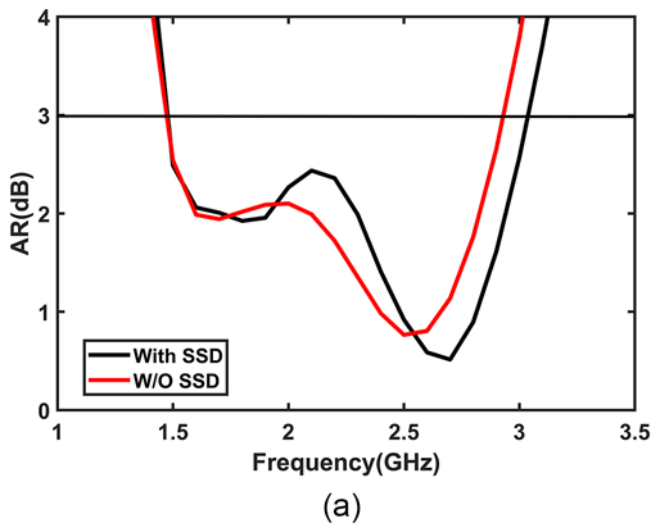


Figure 7. Axial ratio curves of ultimate antenna without SSD and with SSD structures assembling: (a) simulated and (b) measured.

antenna with the previously reported works, which provides excellent performance in the main parameters of the proposed antenna.

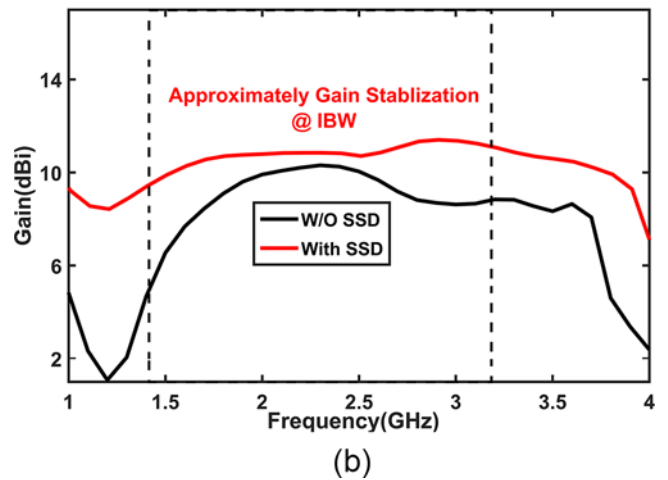
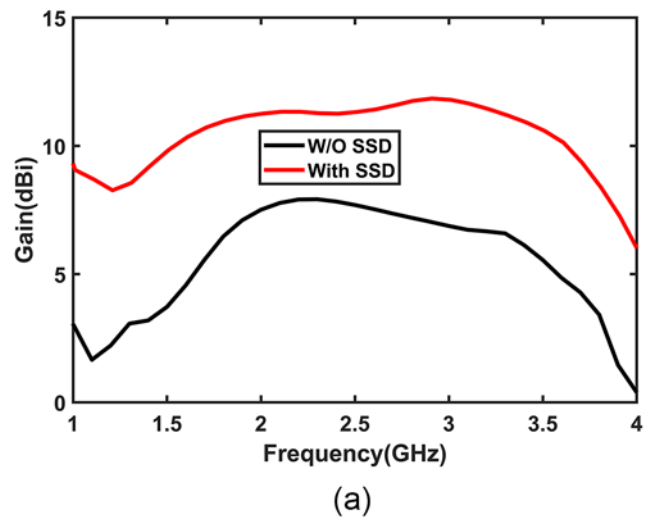


Figure 9. Gain curve of ultimate antenna without SSD and with SSD structures assembling: (a) simulated and (b) measured.

Conclusion

A new broadband antenna structure including a 3D plane and a quarter wavelength vertical resonator was introduced. A structure in the form of SSDs is introduced to increase overall performance of antenna. The proposed structure is excited by a Γ -shaped

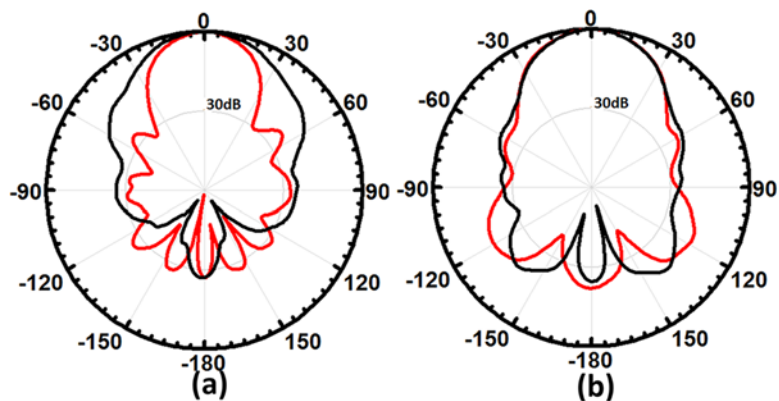


Figure 10. The measured radiation pattern of the proposed antenna: (a) 2.8 GHz and (b) 2.6 GHz.

Note: black: e-field plane and red: H-field plane.

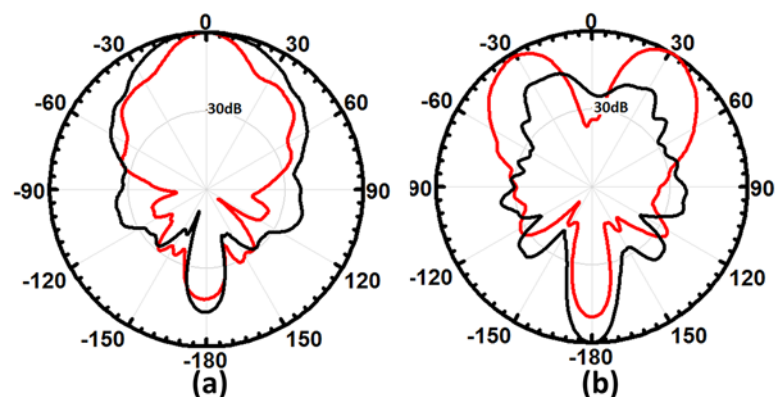


Figure 11. The measured radiation pattern of the circular polarization of the proposed antenna @ 2.8 GHz: (a) right-handed and (b) left-handed.

Table 1. Comparison of the proposal with previously reported works

	%BW	Gain [dB]	HPBW [Deg]	% Polarization purity
[22]	52	8.5	65	N/A
[23]	30.3	9	N/A	18
[21]	60	8.35	165	22
This work	87	13.5	65	98

band line. The impedance bandwidth was 87% and the maximum gain was 13 dB. The property of circular polarization was achieved in 98% of the impedance bandwidth of the antenna. The introduced structure has advantages such as the ease of wide bandwidth design, low cross polarization level, circular polarization and relatively symmetrical radiation patterns and acceptable side lobe level. The gain and beam width of the antenna is almost constant and stable in the entire bandwidth of the antenna. The proposed antenna has applications in the modern wireless telecommunication industry.

Data availability statement. The participants of this study did not give written consent for their data to be shared publicly, so the research supporting data is not available.

Author contributions. All authors' contributed equally to simulations analyzing data and reaching conclusions, and in writing the paper.

Funding statement. This research received no specific grant from any funding agency, commercial or not-for-profit sectors.

Competing interests. The authors report no conflict of interest.

References

1. Mohammadi P and Siah MHRT (2019) A circularly polarized wide-band magneto-electric dipole antenna with simple structure for BTS applications. *AEU - International Journal of Electronics and Communications* **105**, 92–97.
2. Baba A, Hashmi RM and Esselle KP (2016) Wideband gain enhancement of slot antenna using superstructure with optimised axial permittivity variation. *Electronics Letters* **52**(4), 266–268.
3. Hashmi RM, Zeb BA and Esselle KP (2014) Wideband high-gain EBG resonator antennas with small footprints and all-dielectric superstructures. *IEEE Transactions on Antennas and Propagation* **62**(6), 2970–2977.
4. Hashmi RM and Esselle KP (2016) A class of extremely wideband resonant cavity antennas with large directivity-bandwidth products. *IEEE Transactions on Antennas and Propagation* **64**(2), 830–835.
5. Wang N, Li J, Wei G, Talbi L, Zeng Q and Xu J (2015) Wideband Fabry Perot resonator antenna with two layers of dielectric superstrates. *IEEE Antennas and Wireless Propagation Letters* **14**, 229–232.
6. Ge Y, Sun Z and Chen YY (2016) A high-gain wideband low-profile Fabry-Perot resonator antenna with a conical short horn. *IEEE Antennas and Wireless Propagation Letters* **15**, 1889–1892.
7. Chacko BP, Augustin G and Denidni TA (2016) FPC antennas: C-band point-to-point communication systems. *IEEE Antennas and Propagation Magazine* **58**(1), 56–64.
8. Wu F and Luk KM (2017) Wideband high-gain open resonator antenna using a spherically modified, second-order cavity. *IEEE Transactions on Antennas and Propagation* **65**(4), 2112–2116.
9. Baba A, Hashmi RM and Esselle KP (2017) Achieving a large gain-bandwidth product from a compact antenna. *IEEE Transactions on Antennas and Propagation* **65**(7), 3437–3446.
10. Kovaleva M, Bulger D, Zeb BA and Esselle KP (2017) Cross-entropy method for electromagnetic optimization with constraints and mixed variables. *IEEE Transactions on Antennas and Propagation* **65**(10), 5532–5540.

11. **Khalily M, Tafazolli R, Xiao P and Kishk AA** (2018) Broadband mm-wave microstrip array antenna with improved radiation characteristics for different 5G applications. *IEEE Transactions on Antennas and Propagation* **66**(9), 4641–4647.
12. **Xu H, Zhou J, Wu Q, Hong W and Hong W** (2018) Planar wide-band circularly polarized cavity-backed stacked patch antenna array for millimeter-wave applications. *IEEE Transactions on Antennas and Propagation* **66**(10), 5170–5179.
13. **Zhang Y, Hong W and Mittra R** (2019) 45 GHz wideband circularly polarized planar antenna array using inclined slots in modified short-circuited SIW. *IEEE Transactions on Antennas and Propagation* **67**(3), 1669–1680.
14. **Zhang L, Wu K, Wong SW, He Y, Chu P, Li W, Wang KX and Gao S** (2020) Wideband high-efficiency circularly polarized SIW-fed S-dipole array for millimeter-wave applications. *IEEE Transactions on Antennas and Propagation* **68**(3), 2422–2427.
15. **Xu J, Hong W, Jiang ZH, Zhang H and Wu K** (2020) Low-profile wide-band vertically folded slotted circular patch array for Ka-band applications. *IEEE Transactions on Antennas and Propagation* **68**(9), 6844–6849.
16. **Sedghi T, Shafei S, Kalami A and Aribi T** (2015) Small monopole antenna for IEEE 802.11a and X-Bands applications using modified CBP structure. *Wireless Personal Communications* **80**, 859–865.
17. **Li T and Chen ZN** (2020) Wideband sidelobe-level reduced K a-band meta surface antenna array fed by substrate-integrated gap waveguide using characteristic mode analysis. *IEEE Transactions on Antennas and Propagation* **68**(3), 1356–1365.
18. **Yin J, Wu Q, Yu C, Wang H and Hong W** (2019) Broadband symmetrical E-shaped patch antenna with multimode resonance for 5G millimeter-wave applications. *IEEE Transactions on Antennas and Propagation* **67**(7), 4474–4483.
19. **Heidari F, Adelpoure Z and Parhizgar N** (2022) Simulation of leaky wave antenna with cosecant squared pattern using genetic algorithm. *Journal of Communication Engineering* **11**(42), 69–76.
20. **Sun G-H and Wong H** (2020) A planar millimeter-wave antenna array with a pillbox-distributed network. *IEEE Transactions on Antennas and Propagation* **68**(5), 3664–3672.
21. **Rezvani M and Mohammadi P** (2019) A dual-polarized reflector antenna with $\lambda/2$ printed dipoles for femtocell applications. *Journal of Instrumentation* **14**, P02004.
22. **Wen D-L, Zheng D-Z and Chu Q-X** (2017) A wideband differentially fed dual-polarized antenna with stable radiation pattern for base stations. *IEEE Transactions on Antennas and Propagation* **65**, 2248–2255.
23. **Ni D, Yang S, Chen Y and Song Z** (2017) Extremely low-profile wideband dual-polarized microstrip antenna for micro-base-station applications. *International Journal of RF and Microwave Computer-Aided Engineering* **27**, 1–8.



Seied Ali Banihashem received the M.S. degree in telecommunication engineering from Islamic Azad University, Urmia, Iran, in 2015, where he is currently pursuing the Ph.D. degree in electrical and telecommunications. His current research interest includes patch antenna array with fan-beam characteristics.



Pejman Mohammadi received the Ph.D. degree in electrical engineering from the Middle East Technical University Turkey, Ankara, Turkey, in 2012. Since 2001, he has been with the Department of Electrical Engineering, Islamic Azad University, Urmia Branch, Urmia, Iran, where he is currently an Associate Professor. His research interests include microwave component substrate-integrated waveguide (SIW), microwave sensors, microstrip antennas, small antennas for wireless communications, and reconfigurable structures. Dr Mohammadi is a member of the Microwave and Antenna Research Center, Islamic Azad University, Urmia Branch.



Yashar Zehforoosh was born in Urmia, Iran, in 1981. He received the M.S. degree from Urmia University, Urmia, in 2007, and the Ph.D. degree in telecommunication engineering from the Science and Research Branch, Islamic Azad University, Tehran, Iran, in 2012. He is currently an Associate Professor with the Department of Electrical Engineering, Islamic Azad University, Urmia Branch, Urmia. He is also the Head of the Microwave and Antenna Research Center, Islamic Azad University, Urmia Branch. His current research interests include microwave, electromagnetic components, MIMO systems, and antennas.